Journal of Photochemistry and Photobiology A: Chemistry 220 (2011) 179–187

Contents lists available at ScienceDirect

Journal of Photochemistry and Photobiology A: Chemistry

journal homepage: www.elsevier.com/locate/jphotochem

Orientation and organization of gold nanorods on a substrate using a strong magnetic field: Effect of aspect ratio

Hiroaki Yonemura [a,*], Sakai Natsuko [b], Junichi Suyama [b], Sunao Yamada [a]

[a] Department of Applied Chemistry, Faculty of Engineering, Kyushu University, 744 Motooka, Nishi-ku, Fukuoka 819-0395, Japan
[b] Department of Materials Physics and Chemistry, Graduate School of Engineering, Kyushu University, 744 Motooka, Nishi-ku, Fukuoka 819-0395, Japan

ARTICLE INFO

Article history:
Received 31 January 2011
Received in revised form 12 March 2011
Accepted 2 April 2011
Available online 12 April 2011

Keywords:
Gold nanorod
Surface plasmon
Aspect ratio
Side-by-side aggregation
Magnetic orientation
Magnetic organization

ABSTRACT

The effects of magnetic processing on the orientation and the organization of three different types of gold nanorods (AuNRs) [l-AuNR (aspect ratio (AR) = 8.3), m-AuNR (AR = 5.0), and s-AuNR (AR = 2.5)] using a strong magnetic field were investigated. This investigation was performed using the extinction and the polarized extinction spectra that correspond to surface plasmons on a glass plate, and scanning electron microscopy (SEM). For m-AuNR, the results obtained from the extinction spectra and SEM images showed that a side-by-side aggregation of AuNRs formed in the presence of a magnetic field (10 T). In the absence of the magnetic field, side-by-side AuNRs aggregates were not observed. The polarized extinction spectra and the SEM images on the plates indicated that the long axes of AuNRs were oriented parallel to the magnetic field. Similar effects of magnetic processing on the orientation and the organization of AuNRs were observed in the l-AuNR. The magnitude of magnetic orientation in the l-AuNR was larger than that in the m-AuNR. No orientation or organization effects for the s-AuNRs on glass plates were observed. The effect of AR on the magnetic orientation of three AuNRs confirms that the magnetic orientation of AuNRs is because of the anisotropy in the magnetic susceptibilities of the adsorbed CTAB on AuNRs. When the magnetic processing was performed using the dilute concentration of aqueous solutions of m-AuNR, the opposite magnetic orientation, that the long axes of m-AuNRs were oriented perpendicular to the magnetic field, was obtained. The magnetic orientation is probably responsible for the magnetic property of the pristine m-AuNR.

1. Introduction

The application of strong magnetic fields on materials induces strong magnetic-field effects. This can lead to the creation of highly functional nanomaterials with new properties, which result from the new interfaces or nanostructures formed by the strong magnetic fields [1].

The magnetic orientation of crystals [2], polymers [3], fibrin fiber [4,5], and carbon nanotubes [6,7] by strong magnetic fields using a superconducting magnet has been widely investigated. 2D- and 3D-patterns in silver dendrites in a strong magnetic field were reported [8,9]. Significant morphological changes induced by magnetic fields were interpreted in terms of the magnetohydrodynamic mechanism. In this process the Lorentz force and/or a magnetic force that is caused by a gradient magnetic field affects the motions of ions in a magnetic field. Magnetic field effects (MFEs) on growth morphology in electropolymerization, photoelectrochemical reactions, and the redox behaviors of the conducting polymer, polypyrrole, have been reported by Mogi et al. [10,11]. The MFEs were explained via the diamagnetic orientation of the polymers. Recently, Tanimoto et al. reported 3D morphological chirality in membrane tubes prepared through a silicate garden reaction using a strong magnetic field [12,13].

We have reported the effects of magnetic processing on the morphological, electrochemical, and photoelectrochemical properties of electrodes modified with nanoclusters of phenothiazine-C_{60} systems [14–16]. Recently, we have also reported that the magnetic orientation of nanowires consisting of regioregular poly(3-alkylthiophene) (poly(3-hexylthiophene) [17] and poly(3-butylthiophene) [18]).

Gold nanorods (AuNRs) possess unique optical properties that are dependent on the size and the aspect ratio (AR: the ratio of the longitudinal-to-transverse length). A spherical gold nanoparticle has only one localized surface plasmon (SP) band in the visible region. By contrast, AuNRs have a couple of localized SP bands. One localized SP band corresponds to the transverse oscillation mode, which absorbs in the visible region around 520 nm. However, the other SP band corresponds to the longitudinal oscillation mode that absorbs in the far- to near-infrared region. The localized SP resonance properties can be tuned via the AR of the AuNR [19].

* Corresponding author. Tel.: +81 92 802 2814; fax: +81 92 802 2815.
E-mail address: yonemura@mail.cstm.kyushu-u.ac.jp (H. Yonemura).

1010-6030/$ – see front matter © 2011 Elsevier B.V. All rights reserved.
doi:10.1016/j.jphotochem.2011.04.010

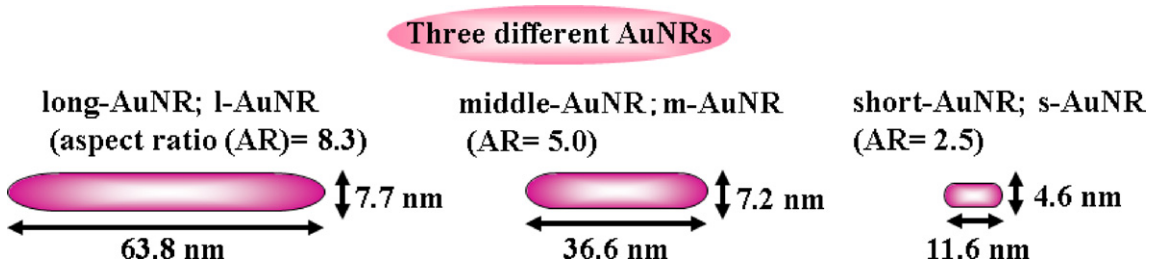

Fig. 1. Three different types of gold nanorods (AuNRs).

The AuNRs have a high sensitivity to the dielectric constant of the surrounding medium (e.g. solvent, substrates, adsorbents and the inter-distances of AuNRs) [20–25]. In addition, the localized SP resonance properties caused by inter-SP coupling are influenced by the orientations of the AuNRs, which include side-by-side, end-to-end and side-to-end structures [21–25].

Recently, we reported the effects of magnetic processing on the orientation and the organization of AuNR/poly(styrenesulfonate) (PSS) composites on a substrate [26]. The magnetic processing resulted in magnetic organization via the side-by-side aggregation of some AuNR/PSS composites and the long axes of AuNRs oriented parallel to the magnetic field. The magnetic orientation is most likely because of the anisotropy in the magnetic susceptibilities of the adsorbed hexadecyltrimethylammonium bromide (CTAB) on AuNRs.

However, the role of PSS in the orientation and organization of AuNR/PSS composites has not yet been explained. Also, the effects of AR on the magnetic orientation and organization of AuNRs have not yet been examined. In this study, we examined the effects of AR on the magnetic processing, organization and orientation of AuNRs on a substrate using three AuNRs with different ARs to identify the mechanisms involved.

2. Experimental

AuNRs were prepared using modifications to the previously reported method [27]. The AuNRs were supplied by Dai Nippon Toryo Co. Ltd. (Osaka, Japan) and Mitsubishi Materials Co. Ltd. (Tokyo, Japan). Three different types of AuNRs (l-AuNR, m-AuNR, and s-AuNR) were used (Fig. 1). The average length and width of the AuNRs were 63.8 and 7.7 nm for the l-AuNRs; 36.6 and 7.2 nm for the m-AuNRs; and 11.6 and 4.6 nm for the s-AuNRs. Therefore, the ARs of l-AuNR, m-AuNR, and s-AuNR are 8.3, 5.0 and 2.5, respectively. The AR of the m-AuNR is same as that of the AuNRs in the AuNR/PSS composites [26].

The AuNRs in aqueous solution contain an excess amount of CTAB, which serves as a stabilizing agent. Centrifugation (7000 rpm, 15 min; l-AuNR, 15,000 rpm, 20 min; m-AuNR, and 20,000 rpm, 30 min; s-AuNR) of the aqueous AuNRs solution was carried out twice to remove the excess CTAB.

Magnetic processing of the samples was performed using a superconducting magnet with a vertical (B_{max} = 10 T) magnetic field [16,18,26]. A superconducting magnet (Oxford Instruments, LOW loss 10 T High field solenoid system S10-76.5 (60 RT)-B, Oxfordshire, UK) with a vertical magnetic field was used [16,18,26]. The magnet had a tube bore width of 60 mm without the aluminum thermostat present, and a bore width of 40 mm with the thermostat. The maximum field (B_{max}(vertical)) and field (B) × gradient field (dB/dz) were 10 T and 485 T^2/m, respectively, where z is the distance from the center of the bore tube. The samples were placed at the middle position (10 T and 0 T^2/m). For comparison, a sample was placed outside the tube. The temperatures of the samples in the absence and the presence of the magnetic field were kept constant using a temperature regulated circulating water-bath system (NESLAB RTE-8, Thermo Scientific, Waltham, MA).

Magnetic processing of the samples was performed using the component of the magnetic field parallel to the surface of the glass or ITO plate (Fig. 2). The glass plates were made hydrophilic via treatment with a mixed solution (1:1) of aqueous hydrogen peroxide (31%) and ammonia (28%). The ITO plates were cleaned via washing in acetone and methanol, and ozone exposure. In Fig. 2, the glass or ITO plate was immersed in an aqueous solution of AuNR (l-AuNR, m-AuNR, or s-AuNR). In the vessel the magnetic processing was performed using a magnetic field that was directed parallel to the sample surface. In effects of magnetic processing on the m-AuNRs on a substrate, two concentrations of aqueous solutions of m-AuNR, such that the extinction of SP band at 914 nm were 0.1 (Fig. 3) and 0.05, were prepared. In effects of AR on the magnetic processing of AuNRs on substrates, the concentrations of three aqueous solutions of AuNRs, such that the extinction of SP band at their corresponding peak wavelengths (l-AuNR; 1292 nm, m-AuNR; 914 nm, or s-AuNR; 710 nm) was 0.1 (Fig. 3), were prepared. After evaporating water at 323 K at atmospheric pressure, SEM measurement of the sample on the ITO plates, and extinction spectra or polarized extinction spectra measurements of the samples on the glass plates were performed. SEM images were obtained using

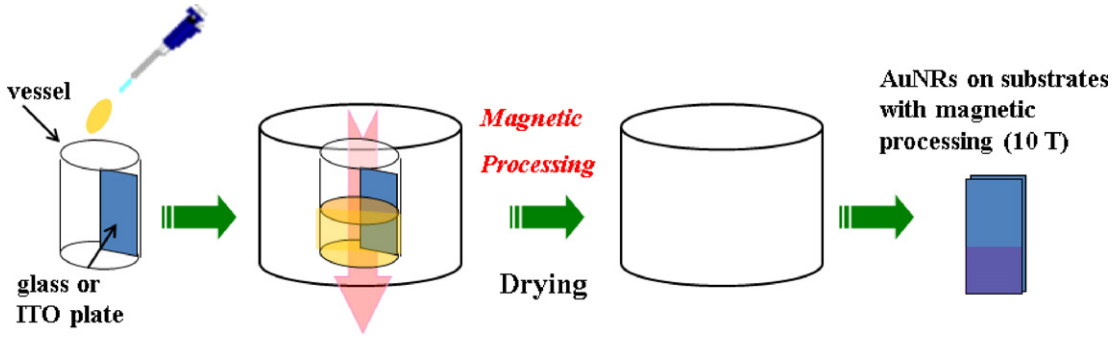

Fig. 2. Schematic of the magnetic processing (10 T).

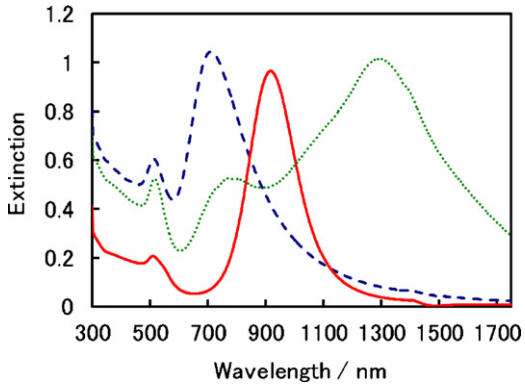

Fig. 3. Extinction spectra of l-AuNR (green dotted line), m-AuNR (red solid line), and s-AuNR (blue dashed line) in aqueous solutions at room temperature. (For interpretation of the references to color in this figure legend, the reader is referred to the web version of the article.)

a Hitachi S-5000 microscope. Steady-state and polarized extinction spectra of the solutions or glass plates were recorded using a UV–VIS–NIR scanning spectrometer (Shimadzu UV-3150, Kyoto, Japan), a polarizer (Assy III; 260–2500 nm) and a sample immobilization set of glass plates (Shimadzu P/N 206-81042) at room temperature [7,17,18,26].

3. Results and discussion

3.1. Characterization of three AuNRs

The SP bands of the aqueous solutions of three l-AuNR, m-AuNR, and s-AuNR following centrifugation are shown in Fig. 3. In the figure, two SP bands of m-AuNR and s-AuNR, and three SP bands for l-AuNR can be seen. In the l-AuNR, the SP band in the visible region at 515 nm represents the transverse oscillation mode. The stronger SP band corresponds to the longitudinal oscillation mode at 1292 nm. The weaker SP band at 769 nm corresponds to the longitudinal oscillation mode of the small amount of shorter AuNRs present the l-AuNR. In the m-AuNR, the SP band in the visible region at 509 nm represents the transverse oscillation mode, and the stronger SP band corresponds to the longitudinal oscillation mode at 914 nm. These results for the m-AuNR are in fair agreement with those in our previous paper [26]. In the s-AuNR, the SP band in the visible region at 515 nm represents the transverse oscillation mode, and the stronger SP band corresponds to the longitudinal oscillation mode at 710 nm. The peak of SP band corresponding to the longitudinal mode drastically increases with increasing AR, which can be seen in Fig. 3 [19]. However, the peak of SP band that corresponds to the transverse mode changes little with increasing AR.

3.2. Effects of magnetic processing on the m-AuNRs on a substrate

The extinction spectra and polarized extinction spectra of the three types of AuNRs on glass plates were measured. The spectra were acquired to investigate the magnetic organization and orientation of the AuNRs, which has been previously reported for single carbon nanotubes [7], their composites [7], polythiophene nanowires [17,18] and AuNR/PSS composites [26].

We examined the extinction spectra and the polarized extinction spectra of the m-AuNR on glass plates to investigate the role of PSS in magnetic processing on the AuNR/PSS composites [26]. First, we carried out magnetic processing using normal concentration of aqueous solutions of m-AuNR (Extinction = 0.1, at 914 nm) as similar to AuNR/PSS composites in the previous paper [26]. In the extinction spectrum of the m-AuNR on the glass plate, two SP bands (560 and 1031 nm) corresponding to the transverse and the longitudinal modes were observed in the absence of magnetic processing at 323 K (Fig. 4). An extinction band in the 1200–1750 nm region was barely visible (Fig. 3). The extinction band in the near-infrared region (800–1200 nm) was broadened when compared with the same band in the aqueous solution of m-AuNR (Fig. 3). These results indicate that end-to-end and side-to-end aggregations, but not side-by-side aggregations of AuNRs are present in the absence of a magnetic field [28]. However, the profile of the extinction spectrum of m-AuNR on a glass plate in the absence of magnetic processing was similar to the spectrum recorded for the species in aqueous solution (Fig. 3).

By contrast, in the presence of magnetic processing (10 T) at 323 K, the extinction spectrum of the m-AuNR was drastically different from the spectra observed for m-AuNR samples in the absence of magnetic processing on the glass plate (Fig. 4) and in the aqueous solution (Fig. 3). The peak of the SP band corresponding to the longitudinal mode was observed at 888 nm and significantly blue-shifted compared with that (1031 nm) in the absence of magnetic processing (Fig. 4). Conversely, the peak in the SP band corresponding to the transverse mode was observed at 574 nm and was red-shifted compared with the band observed (560 nm) in the absence of magnetic processing (Fig. 4). In the presence of magnetic processing the absorbance of SP corresponding to the transverse mode was stronger than that corresponding to the longitudinal mode. By contrast, the extinction of the SP corresponding to the transverse mode was noticeably weaker than that of the SP corresponding to the longitudinal mode for the species examined in the absence of magnetic processing in the glass plate (Fig. 4) and in solution (Fig. 3).

The simulated optical spectra corresponding to the longitudinal and transverse oscillation modes of SP in AuNRs were generated using the discrete dipole approximation method, which has been previously described [21]. In this paper, in the presence of side-by-side orientation, the longitudinal SP band was found to be blue-shifted, and this was attributed to the coupling of the plasmons in neighboring AuNRs. The blue-shift increases with decreasing neighboring AuNR distance. Furthermore, simulations have shown that larger blue-shifts in the longitudinal SP band occur in trimer versus dimer AuNRs. The coupling of plasmon of the transverse SP in neighboring AuNRs leads to a red-shift. Moreover, the larger red-shift observed for the AuNR trimers of the transverse SP band was accompanied by larger extinction efficiency in comparison with AuNR dimers. According to previous theoretical studies of the plasmon resonance spectra of inter-AuNRs [21–25], a significant blue-shift of more than 100 nm in the SP band corresponding

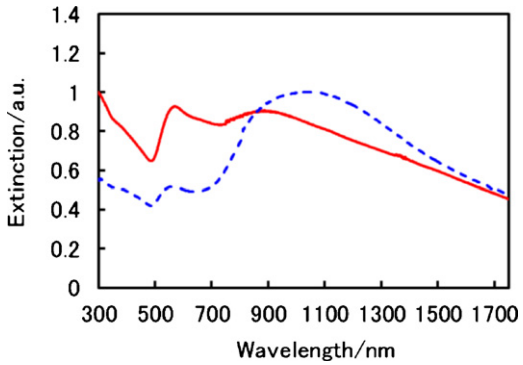

Fig. 4. Normalized extinction spectra of m-AuNR in the absence of magnetic processing (blue dashed line) and the presence of magnetic processing (10 T; red solid line) on glass plate by using the aqueous solution of m-AuNR (concentration: Extinction = 0.1 at 914 nm). (For interpretation of the references to color in this figure legend, the reader is referred to the web version of the article.)

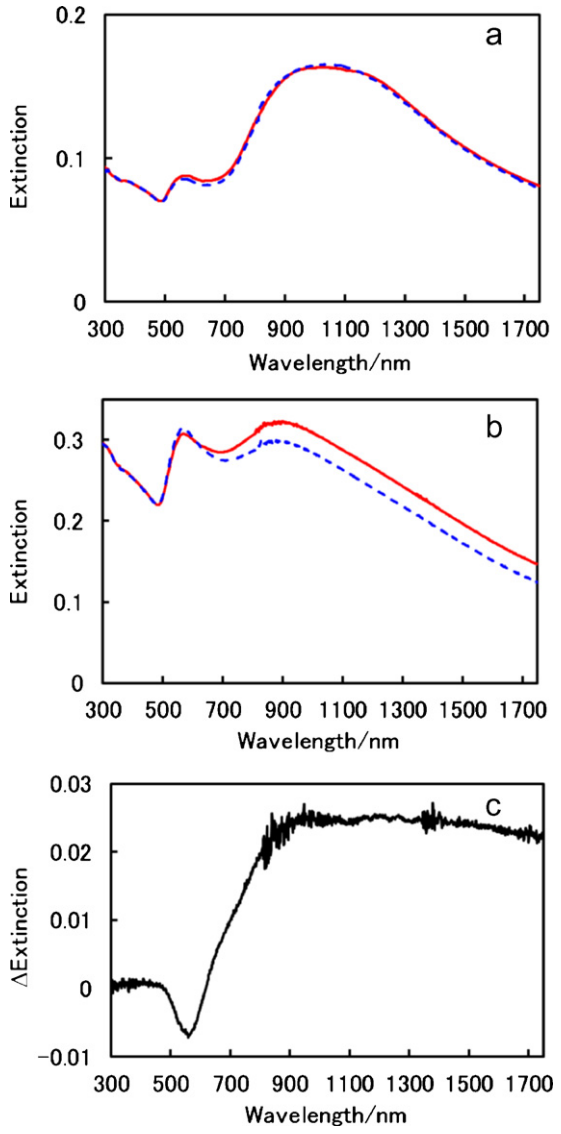

Fig. 5. Polarized extinction spectra for m-AuNR in (a) the absence of magnetic processing and (b) the presence of magnetic processing (10 T) at 323 K. In the absence of magnetic processing, both polarization parallel (red solid line) and perpendicular (blue dashed line) to gravity were investigated. In the presence of magnetic processing (10 T), the polarization direction of the light is parallel ($B(//)$; red solid line) or perpendicular ($B(\perp)$; blue dashed line) to the applied magnetic-field direction on glass plate by using the aqueous solution of m-AuNR (concentration: Extinction = 0.1 at 914 nm). (c) The difference polarized extinction spectrum (ΔExtinction = Extinction($B(//)$) – Extinction($B((\perp)$) derived from the polarizations parallel and perpendicular to the magnetic field. (For interpretation of the references to color in this figure legend, the reader is referred to the web version of the article.)

to the longitudinal mode is expected when the presence of side-by-side interactions when the neighboring AuNR distance is less than 10 nm. The features in extinction spectra in the presence of magnetic processing (Fig. 4) are most likely a result of inter-plasmon coupling because of side-by-side aggregation of m-AuNR. The effect of magnetic processing on the organization of m-AuNR (Fig. 4) is essentially same as that in the AuNR/PSS with AuNRs of the same AR(=5.0) [26].

Polarized extinction spectra for the m-AuNR on glass plates were measured to study the magnetic orientation of the m-AuNR. Fig. 5 shows the polarized extinction spectra of the m-AuNRs on glass plates in the absence and presence of magnetic processing. In Fig. 5(a), the two SP bands of m-AuNR were approximately the same for both polarization directions (parallel and perpendicular) in the absence of magnetic processing. However, the extinction band of the longitudinal SP (800–1750 nm) of the m-AuNRs on the glass plates with the polarization direction parallel to the magnetic field ($B(//)$) was larger than that with the polarization direction perpendicular to the magnetic field ($B(\perp)$) after magnetic processing (10 T). This can be seen in Fig. 5(b). In addition, the extinction band of the transverse SP with the polarization direction parallel to the magnetic field ($B(//)$) was appreciably weaker than that with the polarization direction perpendicular to the magnetic field ($B(\perp)$) (Fig. 5(b)). In the difference polarized extinction spectrum (ΔExtinction = Extinction($B(//)$) – Extinction($B((\perp)$), the extinction band of the longitudinal SP (620–1750 nm) yielded a positive value for ΔExtinction, while the extinction band of the transverse SP (475–620 nm) yielded a negative value for ΔExtinction (Fig. 5(c)). The peak near 947 nm and the dip near 560 nm probably arise from the large side-by-side aggregation of the m-AuNRs. The results, which are presented in Fig. 5, strongly indicate that the long axes of m-AuNRs orient parallel to the magnetic field. The results in Fig. 5 are consistent with those of the AuNR/PSS composites [26]. Through comparison of the results between the m-AuNRs and the AuNR/PSS composites [26], it is clear that the effects of magnetic processing on the magnetic organization and orientation of the AuNR/PSS composites are caused by the AuNRs not the PSS.

Fig. 6 shows SEM images of m-AuNRs on ITO plates in (a) the absence and (b) presence of magnetic processing (10 T). In the absence of magnetic processing, random orientation of the AuNRs was observed (Fig. 6(a)). By contrast, magnetic orientation of m-AuNR was observed in the presence of magnetic processing. The long axes of m-AuNRs in the large side-by-side aggregates of the AuNRs were oriented parallel to the magnetic field (Fig. 6(b)). The results seen in the SEM images are in fair agreement with those of the extinction spectra (Fig. 4) and the polarized extinction spectra (Fig. 5). All of these experimental results strongly indicate the formation of side-by-side aggregates of many m-AuNRs, which the long axes of the m-AuNRs are oriented parallel to the magnetic field used for processing.

Next, we carried out magnetic processing using dilute concentration of aqueous solutions of m-AuNR (Extinction = 0.05, at 914 nm). In the extinction spectrum of the m-AuNR on the glass plate, two SP bands (559 and 978 nm) corresponding to the transverse and the longitudinal modes were observed in the absence of magnetic processing at 323 K (Fig. 7). The profile of the extinction spectrum of m-AuNR on a glass plate in the absence of magnetic processing was similar to the spectrum recorded for the species in aqueous solution (Fig. 3), as similar to that in Fig. 4.

In the presence of magnetic processing (10 T) at 323 K, the extinction spectrum of the m-AuNR was different from the spectra observed for m-AuNR samples in the absence of magnetic processing on the glass plate (Fig. 7). The peak of the SP band corresponding to the longitudinal mode was observed at 946 nm and significantly blue-shifted compared with that (978 nm) in the absence of magnetic processing (Fig. 4). Conversely, the peak in the SP band corresponding to the transverse mode was observed at 550 nm and was also blue-shifted compared with the band observed (559 nm) in the absence of magnetic processing (Fig. 7). In Fig. 7, the drastic change of the spectral shape and the peak shifts of the SP bands corresponding to both the longitudinal and transverse modes were not observed as compared with those in Fig. 4. The ratio of the extinction of the longitudinal and the transverse mode at the peaks (R(B = 10 T) = Extinction(978 nm)/Extinction(559 nm) = 1.23) in the presence of magnetic processing was smaller than that (R(B = 0 T) = Extinction(946 nm)/Extinction(550 nm) = 1.35) in the absence and the presence of magnetic processing.

From similar discussion in Fig. 4, these properties in the extinction spectra in the presence of magnetic processing (Fig. 7) are

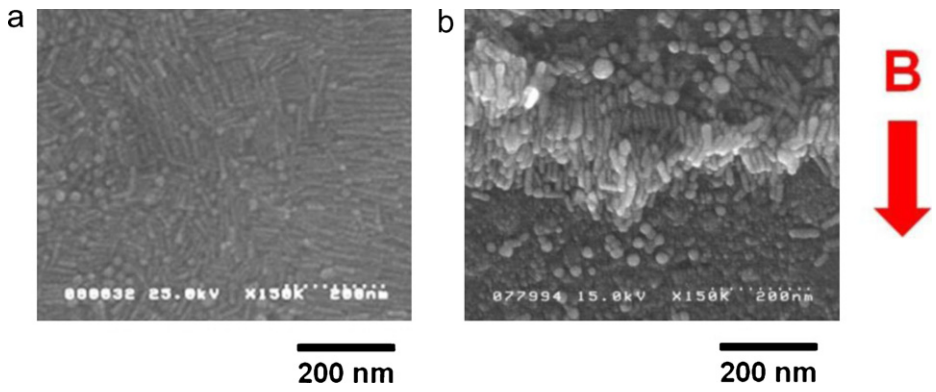

Fig. 6. SEM images of m-AuNRs on ITO plates in (a) the absence and (b) presence of magnetic processing (10 T).

most likely a result of inter-plasmon coupling because of side-by-side aggregation of m-AuNRs. The effect of magnetic processing is essentially same as that in the AuNR/PSS composites [26] and the m-AuNRs (Fig. 4). The magnitude of effect of magnetic processing on the spectral shape and the peak shifts of two SP bands in Fig. 7 is smaller than that in Fig. 4. The results are probably caused by that the neighboring AuNR distance side-by-side aggregation of m-AuNRs in Fig. 7 is long and/or small side-by-side aggregation of m-AuNRs in Fig. 7 forms in Fig. 7 as compared with those in Fig. 4.

Polarized extinction spectra for the m-AuNR on glass plates were also measured to study the magnetic orientation of the m-AuNR as similar to Fig. 5. Fig. 8 shows the polarized extinction spectra of the m-AuNRs on glass plates in the absence and presence of magnetic processing. In Fig. 8(a), the two SP bands of m-AuNR were approximately the same for both polarization directions (parallel and perpendicular) in the absence of magnetic processing. By contrast, the extinction band of the longitudinal SP (800–1750 nm) of the m-AuNRs on the glass plates with the polarization direction perpendicular to the magnetic field ($B(\perp)$) was larger than that with the polarization direction parallel to the magnetic field ($B(//)$) after magnetic processing (10 T) as shown in Fig. 8(b). In addition, the extinction band of the transverse SP with the polarization direction perpendicular to the magnetic field ($B(\perp)$) was appreciably weaker than that with the polarization direction parallel to the magnetic field ($B(//)$) (Fig. 8(b)). In the difference polarized extinction spectrum (ΔExtinction = Extinction($B(//)$) − Extinction($B((\perp)$), the extinction band of the transverse SP (490–580 nm) yielded a positive value for ΔExtinction, while the extinction band of the longitudinal SP (580–1750 nm) yielded a negative value for ΔExtinction (Fig. 8(c)). The peak at 530 nm and the dip near 945 nm

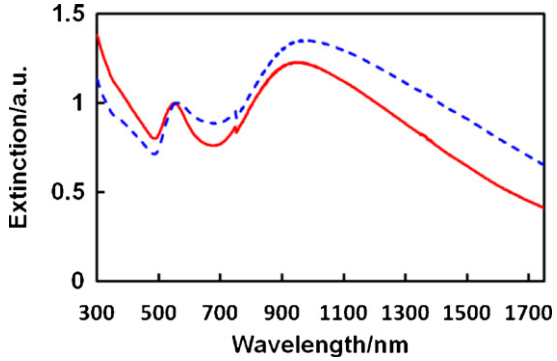

Fig. 7. Normalized extinction spectra for m-AuNR in the absence of magnetic processing (blue dashed line) and the presence of magnetic processing (10 T; red solid line) on glass plate by using the aqueous solution of m-AuNR (concentration: Extinction = 0.05 at 914 nm). (For interpretation of the references to color in this figure legend, the reader is referred to the web version of the article.)

probably arise from the small side-by-side aggregation of them-AuNRs. The results, which are presented in Fig. 8, strongly indicate that the long axes of m-AuNRs orient perpendicular to the magnetic field. Interestingly, the results in Fig. 8 are opposite of those in Fig. 5. Through comparison of the results between Figs. 5 and 8, it is clear that the effects of magnetic processing on the orientation of the m-AuNRs are influenced by the concentration of m-AuNRs, and the m-AuNRs stabilized by CTAB possess two substances with the opposite magnetic orientation each other.

3.3. *Effects of AR on the magnetic processing of AuNRs on substrates*

Next, we examined the effects of AR on the magnetic organization and the magnetic orientation of three AuNRs on glass plates using l-AuNRs and s-AuNRs (AR = 8.3 and 2.5) using normal concentration of aqueous solutions of l-AuNR (Extinction = 0.1, at 1292 nm) and s-AuNR (Extinction = 0.1, at 710 nm).

Fig. 9 shows the extinction spectra of l-AuNR on glass plates in the absence and presence of magnetic processing at 323 K. In the extinction spectrum of l-AuNR, two SP bands (591 and 1564 nm) corresponding to the transverse and the longitudinal modes were observed in the absence of magnetic processing (Fig. 9). The extinction bands corresponding the two SP bands were broadened in the extinction spectra, when compared with the same band in the aqueous solution of l-AuNR (Fig. 3). The broadening of the extinction spectra was attributed to the aggregation of l-AuNRs.

By contrast, the extinction spectrum of the l-AuNR on glass plates in the presence of magnetic processing (10 T) was different from the spectra observed for l-AuNR on glass plate in the absence of magnetic processing (Fig. 9). The peak of the SP band corresponding to the longitudinal mode was observed at 1298 nm. This corresponds to a drastic blue-shift when compared with that (1523 nm) in the absence of magnetic processing (Fig. 9). However, the peak of the SP band corresponding to the transverse mode was observed at 583 nm, which is only a slight blue-shift as compared with the band observed (592 nm) in the absence of magnetic processing (Fig. 7). The ratio of the extinction of the longitudinal and the transverse mode at the peaks (R(B = 10 T) = Extinction(1298 nm)/Extinction(583 nm) = 1.11) in the presence of magnetic processing was smaller than that (R(B = 0 T) = Extinction(1523 nm)/Extinction(592 nm) = 1.25) in the absence and the presence of magnetic processing. These properties in the extinction spectra in the presence of magnetic processing (Fig. 9) are most likely a result of inter-plasmon coupling because of side-by-side aggregation of l-AuNRs. The effect of magnetic processing (Fig. 9) is essentially same as that in the AuNR/PSS composites [26] and the m-AuNRs (Fig. 4).

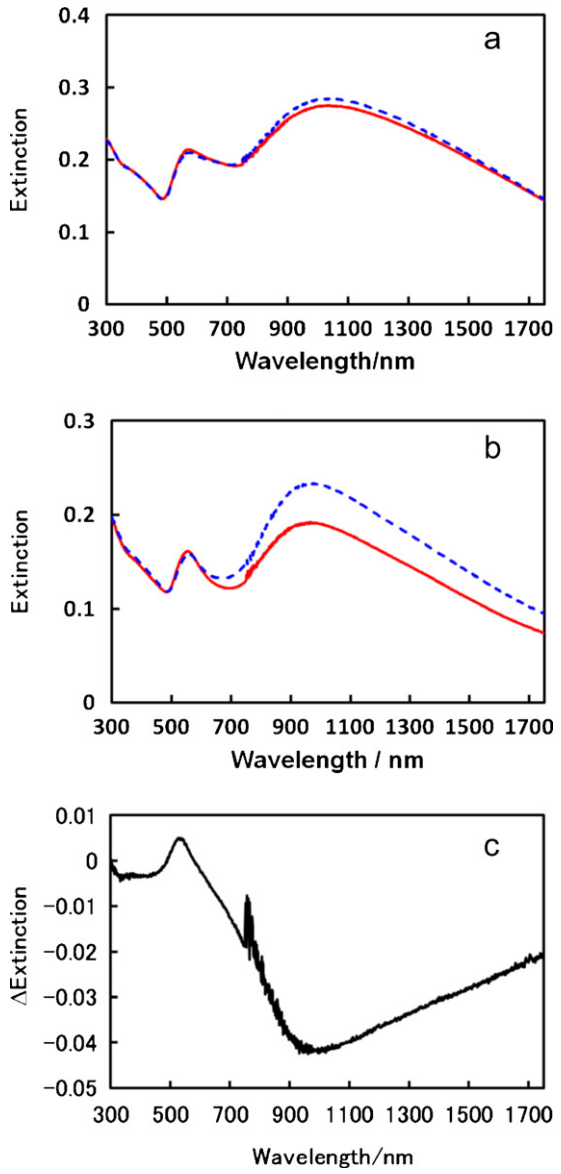

Fig. 8. Polarized extinction spectra for m-AuNR in (a) the absence of magnetic processing and (b) the presence of magnetic processing (10 T) at 323 K. In the absence of magnetic processing, both polarization parallel (red solid line) and perpendicular (blue dashed line) to gravity were investigated. In the presence of magnetic processing (10 T), the polarization direction of the light is parallel ($B(//)$; red solid line) or perpendicular ($B(\perp)$; blue dashed line) to the applied magnetic-field direction on glass plate by using the aqueous solution of m-AuNR (concentration: Extinction = 0.05 at 914 nm). (c) The difference polarized extinction spectrum (ΔExtinction = Extinction($B(//)$) – Extinction($B((\perp)$) derived from the polarizations parallel and perpendicular to the magnetic field. (For interpretation of the references to color in this figure legend, the reader is referred to the web version of the article.)

Polarized extinction spectra of the l-AuNR on glass plates were also measured to study the magnetic orientation of the l-AuNRs (Fig. 10). In Fig. 10(a), two SP bands of m-AuNR were similar in both polarization directions (parallel and perpendicular) in the absence of magnetic processing. However, the extinction band of the longitudinal SP (600–1750 nm) of the l-AuNRs on the glass plates with the polarization direction parallel to the magnetic field ($B(//)$) were larger than that with the polarization direction perpendicular to the magnetic field ($B(\perp)$)in the presence of magnetic processing(10 T). This is shown in Fig. 10(b). Conversely, the extinction band of the transverse SP (480–600 nm) with the polarization direction parallel to the magnetic field ($B(//)$) was appreciably weaker

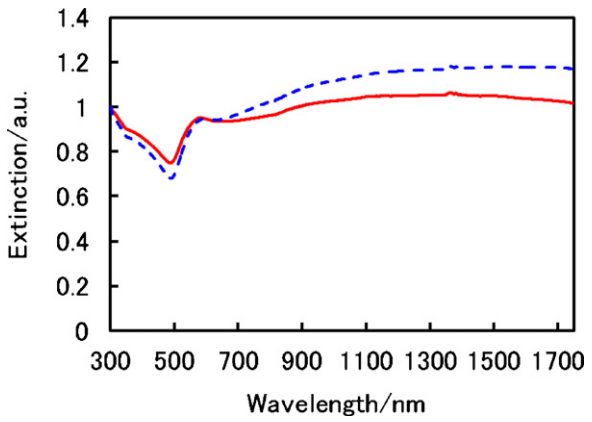

Fig. 9. Normalized extinction spectra for l-AuNR in the absence of magnetic processing (blue dashed line) and the presence of magnetic processing (10 T; red solid line) on glass plate by using the aqueous solution of l-AuNR (concentration: Extinction = 0.1 at 1292 nm). (For interpretation of the references to color in this figure legend, the reader is referred to the web version of the article.)

than that with the polarization direction perpendicular to the magnetic field ($B(\perp)$) in Fig. 10(b). In the difference polarized extinction spectrum (ΔExtinction = Extinction($B(//)$) – Extinction($B((\perp)$), the extinction band of the longitudinal SP (600–1750 nm) had a positive ΔExtinction, while the extinction band of the transverse SP (475–620 nm) had a negative ΔExtinction (Fig. 10(c)). The peak around 1520 nm and the dip around 556 nm probably arise from the large side-by-side aggregation of the l-AuNR. The results in Fig. 10 strongly indicate that the long axes of the l-AuNRs in the large side-by-side aggregates orient parallel to the magnetic field. These results for l-AuNRs are in fair agreement with those for m-AuNRs.

Also, the magnitude of ΔExtinction for the l-AuNRs (Fig. 10(c)) is larger than that for the m-AuNRs (Fig. 5(c)). In other words, the magnitude of magnetic orientation of the l-AuNR is larger than that of the m-AuNR. From this comparison of the results between l-AuNRs and m-AuNRs, the l-AuNRs were more oriented than the m-AuNRs after magnetic processing.

Next, Fig. 11 shows extinction spectra of s-AuNR on glass plates in the absence and presence of magnetic processing at 323 K. In the extinction spectrum of s-AuNR, two SP bands (556 and 845 nm) corresponding to the transverse and the longitudinal modes were observed in the absence of magnetic processing (Fig. 11). The extinction bands because of the two SP bands were broadened when compared with the corresponding bands in the aqueous solution of s-AuNR (Fig. 3). This is similar to the results for both m-AuNRs (Fig. 4) and l-AuNRs (Fig. 9). The broadening of the extinction spectra can be attributed to the aggregation among the s-AuNRs.

By contrast, the extinction spectrum of the s-AuNR on the glass plate in the presence of magnetic processing (10 T) was similar to that observed for s-AuNR on the glass plate in the absence of magnetic processing (Fig. 11). The significant effects of magnetic processing on spectral shape and the peaks due to the two SP bands, which are visible for both m-AuNRs (Fig. 4) and l-AuNRs (Fig. 9), cannot be seen in Fig. 11. In other words, no magnetic organization because of the large side-by-side aggregations of s-AuNR was observed in the case of s-AuNR the glass plates. The results for s-AuNR are different from those for both the m-AuNRs (Fig. 4) and the l-AuNRs (Fig. 9). The difference is probably because of the AR in three AuNRs.

In addition, the polarized extinction spectra of the s-AuNRs on glass plates were also measured to study the magnetic orientation of the s-AuNRs. From Fig. 12, the two SP bands of the s-AuNR were similar in both polarization directions (parallel and perpendicular) in the absence (Fig. 12(a)) and presence of magnetic processing (Fig. 12(b)). These results in Fig. 12 strongly indicate that no mag-

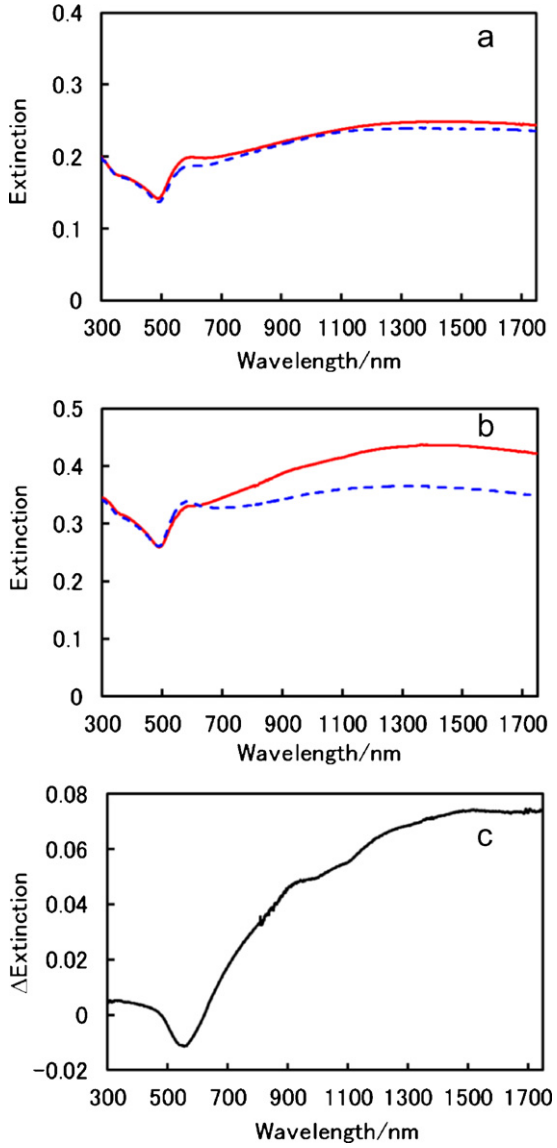

Fig. 10. Polarized extinction spectra of l-AuNR in (a) the absence of magnetic processing and (b) the presence of magnetic processing (10 T) at 323 K. In the absence of magnetic processing, the polarization direction of the light is parallel (red solid line) or perpendicular (blue dashed line) to gravity. In the presence of magnetic processing (10 T), the polarization direction of the light is parallel ($B(//)$; red solid line) or perpendicular ($B(\perp)$; blue dashed line) to the applied magnetic-field direction on glass plate by using the aqueous solution of l-AuNR (concentration: Extinction = 0.1 at 1292 nm). (c) The difference polarized extinction spectrum (ΔExtinction = Extinction($B(//)$) – Extinction($B((\perp)$) derived from the polarizations parallel and perpendicular to the magnetic field. (For interpretation of the references to color in this figure legend, the reader is referred to the web version of the article.)

netic orientation of s-AuNR was observed for s-AuNRs on glass plates.

Some ordered structures such as chain-like alignments and triangle-lattice alignments of gold balls (1 mm, diameters) resulting from magnetic dipole induction from a strong magnetic field have been reported [29]. In our study, despite the nanometer-scale of the AuNRs, we observed magnetic organization in the AuNRs.

Though bulk gold is diamagnetic, it is reported that gold nanoparticle capped with alkylthiol shows paramagnetic [30]. On the other hand, it is known that CTAB is diamagnetic. In our primitive data using SQUID, the powder of m-AuNR stabilized by CTAB shows paramagnetic property in lower magnetic field (<0.8 T), while the powder shows diamagnetic property in

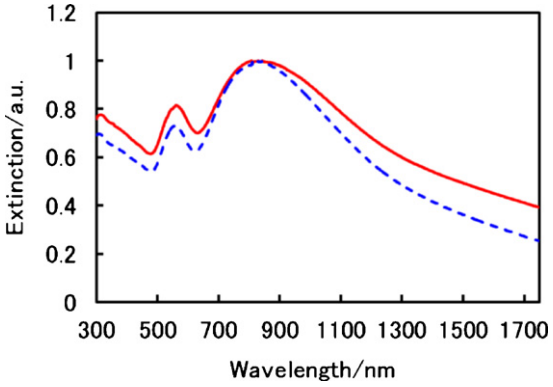

Fig. 11. Normalized extinction spectra of s-AuNR in the absence of magnetic processing (blue broken line) and the presence of magnetic processing (10 T; red solid line) on glass plate by using the aqueous solution of s-AuNR (concentration: Extinction = 0.1 at 710 nm). (For interpretation of the references to color in this figure legend, the reader is referred to the web version of the article.)

higher magnetic field (>0.8 T) at 300 K [31]. The paramagnetic property is attributable to pristine m-AuNR, while the diamagnetic property is attributable to the CTAB as the stabilizing agent.

On the basis of these results, the magnetic orientation in Fig. 8, that the long axes of m-AuNRs orient perpendicular to the magnetic field, is probably responsible for the paramagnetic susceptibility anisotropy of the pristine AuNRs. Therefore, the magnetic organization is probably a result of the magnetic dipoles induced by the strong magnetic field (Fig. 13(a)), which was previously reported in AuNR/PSS composites [26].

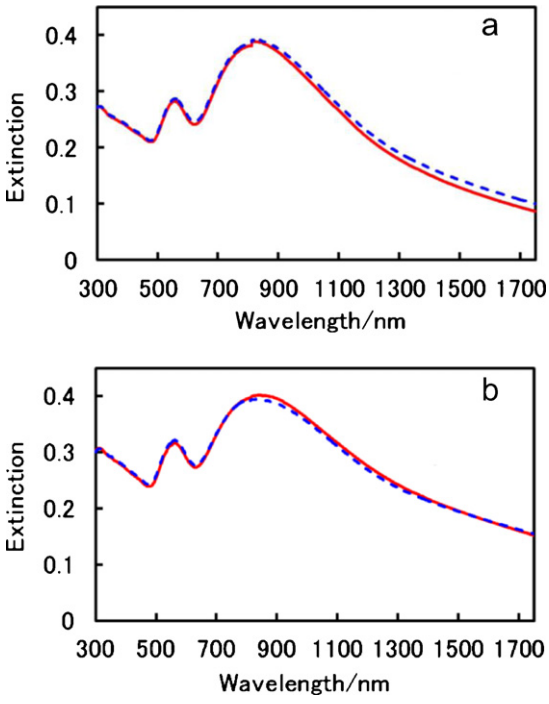

Fig. 12. Polarized extinction spectra of s-AuNR in (a) the absence of magnetic processing and (b) the presence of magnetic processing (10 T) at 323 K. In the absence of magnetic processing, the polarization direction of the light is parallel (red solid line) or perpendicular (blue dashed line) to gravity. In the presence of magnetic processing (10 T), the polarization direction of the light is parallel ($B(//)$; red solid line) or perpendicular ($B(\perp)$; blue dashed line) to the applied magnetic-field direction on glass plate by using the aqueous solution of s-AuNR (concentration: Extinction = 0.1 at 710 nm). (For interpretation of the references to color in this figure legend, the reader is referred to the web version of the article.)

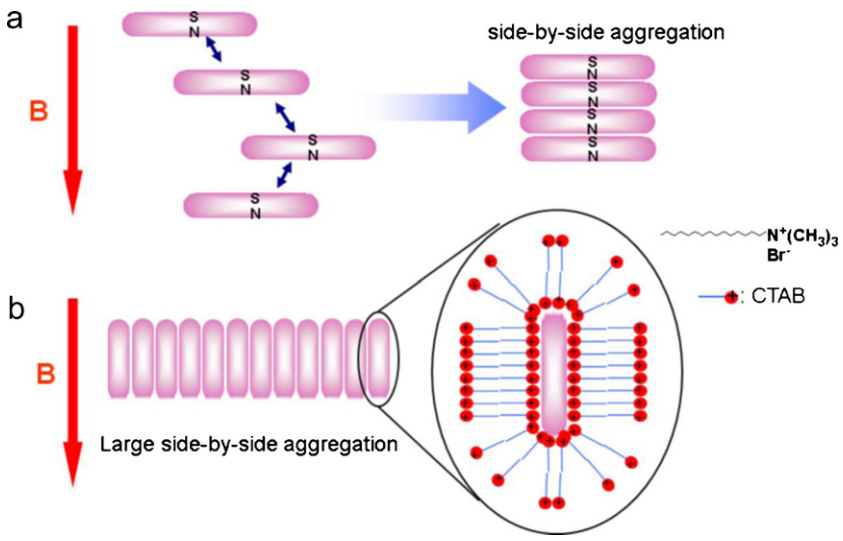

Fig. 13. (a) Proposed mechanism for the side-by-side aggregation of the l- or m-AuNRs induced by the magnetic dipoles in the presence of a magnetic field. (b) The magnetic orientation of the large side-by-side aggregation of the l- or m-AuNRs composites was because of the anisotropy in the magnetic susceptibilities of the adsorbed CTAB that form rod-like micelles on the l- or m-AuNRs.

On the other hand, the magnetic orientation in Figs. 5(b), 8(b) and 10(b), that the long axes of m-AuNRs orient parallel to the magnetic field, is caused by CTAB as a diamagnetic substance. In the previous paper [26], the magnetic orientation could be explained by the anisotropy in the magnetic susceptibilities of the CTAB that formed bilayers on the AuNR/PSS composites [32]. The comparison between the m-AuNRs (Figs. 4 and 5) and the AuNR/PSS composites [26] supports the above explanation. Also, the effects of AR on the magnetic orientation of three types of AuNRs support the above explanation for the reasons described below.

In general, the magnetic orientation via the static magnetic field is caused by the diamagnetic mole susceptibility anisotropy ($\Delta\chi$). Magnetic orientation of a single molecule or a single polymer is not expected to occur at room temperature, because the magnetic energy ($-n\Delta\chi B^2/2$) is negligible compared with the thermal energy (kT). In this case, n, k and T are mole number, the Boltzmann constant and temperature, respectively. However, molecular aggregates, which have an ordered structure like a crystal, can be oriented in a strong magnetic field, because the magnetic energy is greater than the thermal energy at room temperature [1]. In the previous study with the AuNR/PSS composites [26], the magnetic orientation is most likely because of the anisotropy in the magnetic susceptibilities of the adsorbed CTAB on AuNRs. This is similar to the magnetic orientation of mesochannels in mesoporous silica films [33,34]. In this study, the magnetic orientation of l-AuNR and m-AuNR, in which the molecular axis of CTAB is expected to orient perpendicularly to the direction of the magnetic field, can be explained by the anisotropy in the magnetic susceptibilities of the CTAB (Fig. 11). This is similar to the mechanism of the magnetic orientation of the AuNR/PSS composites [26].

An individual CTAB cannot be influenced by a magnetic force, because the magnetic energy associated with $\Delta\chi$ ($-12\pi\times10^{-12}$) for an individual CTAB is relatively small (less than the thermal energy (kT)) in a strong magnetic field (10 T) at 323 K [34]. However, the total magnetic energy overcomes the thermal energy when CTAB molecules form rod-like micelles and align along the direction of the magnetic field. Therefore, if large side-by-side structures form with the combination between the two neighboring AuNRs such as a lamellar structure, the aggregates in which the long axes of the AuNRs are parallel to the magnetic field probably orient as shown in Fig. 13(b). In other words, the magnetic field has no effect on the orientation of the AuNR in the initial stage (individual AuNR), but magnetic orientation occurs once the diamagnetic domain (i.e. CTAB) has reached the critical number for CTAB (i.e. the critical number for AuNR). In this case, large side-by-side aggregations of AuNRs form. The critical numbers for the AuNRs were roughly estimated to be 36, 67, and 329 for l-AuNR, m-AuNR, and s-AuNR, respectively (see Supporting Information) [34]. In the present study, the results for the polarized extinction spectra of l-AuNR, m-AuNR, and s-AuNR suggest that the number of AuNR in the side-by-side aggregates of the AuNRs reached the critical number for l-AuNRs or m-AuNRs in the case of l-AuNR or m-AuNR; however, that critical number was not reached for s-AuNRs.

In the above discussion, we explained that the magnetic orientation of AuNR/PSS composites, l-AuNRs and m-AuNRs is because of the anisotropy in the magnetic susceptibilities of the adsorbed CTABs that form rod-like micelles on AuNRs (Fig. 13(b)).

4. Conclusion

Extinction spectra, polarized extinction spectra, and SEM images of the three AuNRs with different ARs (l-AuNR, m-AuNR, and s-AuNR) on the glass plates and the ITO plates in the absence and presence of magnetic processing showed that magnetic organization. In this case, this was via side-by-side aggregation of many AuNRs. Magnetic orientation of AuNRs could be achieved in l-AuNRs and m-AuNRs, but significant magnetic organization and orientation was not observed in s-AuNR.

The comparison between the m-AuNR and the AuNR/PSS composites [26] and effect of AR on the magnetic orientation of AuNRs confirm that the magnetic orientation of AuNRs is because of the anisotropy in the magnetic susceptibilities of the adsorbed CTAB that form rod-like micelles on AuNRs.

Interestingly, when the magnetic processing using dilute concentration of aqueous solutions of m-AuNR were carried out, the opposite magnetic orientation of m-AuNR, that the long axes of m-AuNRs orient perpendicular to the magnetic field, were observed. The magnetic orientation is most likely attributable to the anisotropy in the magnetic susceptibilities of the pristine m-AuNR. The magnetic orientation due to strong magnetic field can be controlled by the concentration of m-AuNR.

The present results indicate that magnetic processing provide a useful method for the orientation and organization of nanometer-sized aggregates consisting of the mixture of paramagnetic and diamagnetic substances such as the present AuNRs stabilized by

CTAB. Further investigations on the side-by-side aggregation and orientation of the AuNRs or AuNR/PSS composites on glass plates using strong magnetic fields are currently being performed.

Acknowledgments

The authors are grateful to Professor Masahiro Hasuo (Kyoto University) for the use of a superconducting magnet. The authors are also grateful to Professor Nobuo Kimizuka (Kyushu University) for performing SEM measurements. The authors thank to Dr. Daigou Mizoguchi (Dai Nippon Toryo Co. Ltd.) for providing them with three different types of AuNRs. The present study was financially supported by the Mazda Foundation and by a Grant-in-Aid for Scientific Research: Priority Area of "Strong Photons-Molecules Coupling Fields" (Area 470, No. 19049012) and Scientific Research (C) (No. 19022027 and 21550135), Nanotechnology Network Project (Kyushu-area Nanotechnology Network) and the Global COE Program "Science for Future Molecular Systems" from MEXT of Japan.

Appendix A. Supplementary data

Supplementary data associated with this article can be found, in the online version, at doi:10.1016/j.jphotochem.2011.04.010.

References

[1] M. Yamaguchi, Y. Tanimoto (Eds.), Mageneto-Science Magnetic Filed Effects on Materials: Fundamentals and Applications, Kodansha-Springer, 2006.
[2] M. Fujiwara, M. Fukui, Y. Tanimoto, J. Phys. Chem. B 103 (1999) 2627–2630.
[3] T. Kimira, M. Yoshino, T. Yamane, M. Yamato, M. Tobita, Langmuir 20 (2004) 5669–5672.
[4] J. Torbet, J.-M. Freyssinet, G. Hudry-Clergeon, Nature 289 (1981) 91–93.
[5] A. Yamagishi, T. Takeuchi, T. Higashi, M. Date, J. Phys. Soc. Jpn. 58 (1989) 2280–2283.
[6] M. Fujiwara, E. Oki, M. Hamada, Y. Tanimoto, I. Mukouda, Y. Shimomura, J. Phys. Chem. A 105 (2001) 4383–4386.
[7] H. Yonemura, Y. Yamamoto, S. Yamada, Y. Fujiwara, Y. Tanimoto, Sci. Tech. Adv. Mater. 9 (2008), 024213(1–6).
[8] I. Mogi, S. Okubo, Y. Nakagawa, J. Phys. Soc. Jpn. 60 (1991) 3200–3202.
[9] Y. Tanimoto, A. Katsuki, H. Yano, S. Watanabe, J. Phys. Chem. A 101 (1997) 7359–7363.
[10] I. Mogi, K. Watanabe, M. Motooka, Electrochemistry 67 (1999) 1051–1053.
[11] A. Konno, I. Mogi, K. Watanabe, J. Electroanal. Chem. 507 (2001) 202–205.
[12] I. Uechi, A. Katsuki, L. Dunin-Barkovskiy, Y. Tanimoto, J. Phys. Chem. B 108 (2004) 2527–2530.
[13] W. Duan, S. Kitamura, I. Uechi, A. Katsuki, Y. Tanimoto, J. Phys. Chem. B 109 (2005) 13445–13450.
[14] H. Yonemura, Y. Wakita, N. Kuroda, S. Yamada, Y. Fujiwara, Y. Tanimoto, Jpn. J. Appl. Phys. 47 (2008) 1178–1183.
[15] H. Yonemura, Y. Wakita, S. Moribe, S. Yamada, Y. Fujiwara, J. Phys.: Conf. Ser. 156 (2009), 012026 (1–10).
[16] H. Yonemura, Y. Wakita, T. Yamashita, S. Yamada, Thin Solid Films 518 (2009) 668–673.
[17] H. Yonemura, K. Yuno, Y. Yamamoto, S. Yamada, Synth. Met. 159 (2009) 955–960.
[18] H. Yonemura, K. Yuno, S. Yamada, Jpn. J. Appl. Phys. 49 (2010), 01AE06(1–6).
[19] S. Link, Z.L. Wang, M.A. El-Sayed, J. Phys. Chem. B 103 (1999) 3073–3077.
[20] Y. Niidome, H. Takahashi, S. Urakawa, K. Nishioka, S. Yamada, Chem. Lett. 33 (2004) 454–455.
[21] P.K. Jain, S. Eustis, M.A. El-Sayed, J. Phys. Chem. B 110 (2006) 18243–18253.
[22] M. Gluodenis, C.A. Foss Jr., J. Phys. Chem. B 106 (2002) 9484–9489.
[23] H. Nakashima, K. Furukawa, Y. Kashimura, K. Torimitsu, Chem. Commun. 10 (2007) 1080–1082.
[24] Z. Nie, D. Fava, E. Kumacheva, S. Zou, G.C. Walker, M. Rubinstein, Nat. Mater. 6 (2007) 609–614.
[25] Z. Nie, D. Fava, M. Rubinstein, E. Kumacheva, J. Am. Chem. Soc. 130 (2008) 3683–3689.
[26] H. Yonemura, J. Suyama, T. Arakawa, S. Yamada, Thin Solid Films 518 (2009) 799–804.
[27] Y. Niidome, K. Nishioka, H. Kawasaki, S. Yamada, Chem. Commun. 18 (2003) 2376–2377.
[28] X.H. Huang, I.H. El-Sayed, W. Qian, M.A. El-Sayed, J. Am. Chem. Soc. 128 (2006) 2115–2120.
[29] N. Hirota, T. Takayama, E. Beaugnon, Y. Saito, T. Ando, H. Nakamura, S. Hara, Y. Ikezoe, H. Wada, K. Kitazawa, J. Magn. Magn. Mater. 293 (2005) 87–92.
[30] P. Crespo, R. LitrPn, T.C. Rojas, M. Multigner, J.M. de la, Fuente, J.C. SPnchez-LRpez, M.A. GarcSa, A. Hernando, S. PenadTs, A. FernPndez, Phys. Rev. Lett. 93 (2004), 087204(1–4).
[31] H. Yonemura, N. Sakai, T. Inagaki, S. Yamada, in preparation.
[32] B. Nikoobakht, M.A. El-Sayed, Langmuir 17 (2001) 6368–6374.
[33] Y. Yamauchi, M. Sawada, A. Sugiyama, T. Osaka, Y. Sakka, K. Kuroda, J. Mater. Chem. 16 (2006) 3693–3700.
[34] Y. Yamauchi, M. Sawada, A. Sugiyama, T. Osaka, Y. Sakka, K. Kuroda, Chem. Asian J. 2 (2007) 1505–1512.